The Plant Cell, Vol. 30: 481–494, February 2018, www.plantcell.org © 2018 ASPB.

MAC3A and MAC3B, Two Core Subunits of the MOS4-Associated Complex, Positively Influence miRNA Biogenesis

Shengjun Li,[a,b,c] Kan Liu,[b,c] Bangjun Zhou,[b,d] Mu Li,[b,c] Shuxin Zhang,[e] Lirong Zeng,[b,d] Chi Zhang,[b,c] and Bin Yu[b,c,1]

[a] Qingdao Engineering Research Center of Biomass Resources and Environment, Qingdao Institute of Bioenergy and Bioprocess Technology, Chinese Academy of Sciences, Qingdao 266101, China
[b] Center for Plant Science Innovation University of Nebraska-Lincoln, Lincoln, Nebraska 68588-0666
[c] School of Biological Sciences, University of Nebraska-Lincoln, Lincoln, Nebraska 68588-0118
[d] Department of Plant Pathology, University of Nebraska, Lincoln, Nebraska 68583-0722
[e] State Key Laboratory of Crop Biology, College of Life Sciences, Shandong Agricultural University, Taian 271018, China

ORCID IDs: 0000-0003-0469-3222 (S.L.); 0000-0003-2986-6310 (B.Z.); 0000-0001-8802-4872 (L.Z.); 0000-0002-4763-177X (B.Y.)

MAC3A and MAC3B are conserved U-box-containing proteins in eukaryotes. They are subunits of the MOS4-associated complex (MAC) that plays essential roles in plant immunity and development in *Arabidopsis thaliana*. However, their functional mechanisms remain elusive. Here, we show that Arabidopsis MAC3A and MAC3B act redundantly in microRNA (miRNA) biogenesis. Lack of both MAC3A and MAC3B in the *mac3b mac3b* double mutant reduces the accumulation of miRNAs, causing elevated transcript levels of miRNA targets. *mac3a mac3b* also decreases the levels of primary miRNA transcripts (pri-miRNAs). However, MAC3A and MAC3B do not affect the promoter activity of genes encoding miRNAs (*MIR* genes), suggesting that they may not affect *MIR* transcription. This result, together with the fact that MAC3A associates with pri-miRNAs in vivo, indicates that MAC3A and MAC3B may stabilize pri-miRNAs. Furthermore, we find that MAC3A and MAC3B interact with the DCL1 complex that catalyzes miRNA maturation, promote DCL1 activity, and are required for the localization of HYL1, a component of the DCL1 complex. Besides MAC3A and MAC3B, two other MAC subunits, CDC5 and PRL1, also function in miRNA biogenesis. Based on these results, we propose that MAC functions as a complex to control miRNA levels through modulating pri-miRNA transcription, processing, and stability.

INTRODUCTION

MicroRNAs (miRNAs), ~21 nucleotides in size, are endogenous noncoding RNAs that mainly repress gene expression at post-transcriptional levels (Baulcombe, 2004; Axtell, 2013). They are generated from the imperfect stem-loop residing in the primary miRNA transcripts (pri-miRNAs) (Voinnet, 2009), most of which are produced by DNA-dependent RNA polymerase II (Xie et al., 2005). In plants, the RNase III enzyme DICER-LIKE1 (DCL1) slices pri-miRNAs at least two times in the nucleus to release a miRNA-containing duplex (Baulcombe, 2004; Axtell, 2013; Zhang et al., 2015). Then, the small RNA methyltransferase HUA ENHANCER1 (HEN1) methylates the miRNA duplexes to protect them from degradation and untemplated uridine addition (Zhai et al., 2013; Ren et al., 2014). Following methylation, the miRNA strand is incorporated into the effector called ARGONAUTE1 (AGO1) with the assistance from HEAT SHOCK PROTEIN90 and CYCLOPHILIN40 and recognizes target transcripts through sequence complementarity (Baumberger and Baulcombe, 2005; Vaucheret, 2008; Smith et al., 2009; Earley and Poethig, 2011). AGO1 cleaves target mRNAs or inhibits their translation and therefore represses gene expression.

pri-miRNAs may be cotranscriptionally processed since DCL1 associates with *MIR* loci (Fang et al., 2015a). In the past decades, protein factors that regulate miRNA biogenesis through influencing pri-miRNA transcription, processing, and stability have been identified in plants. The transcriptional coactivator MEDIATOR (Kim et al., 2011), the CYCLIN-DEPENDENT KINASEs (CDKs) (Hajheidari et al., 2012), the transcription factor NEGATIVE ON TATA LESS2 (NOT2) (Wang et al., 2013), the DNA binding protein CELL DIVISION CYCLE5 (CDC5) (Zhang et al., 2013), and ELONGATOR (Fang et al., 2015a) are required for optimized Pol II activity at the *MIR* promoters. Following transcription, the forkhead domain-containing protein DAWDLE (DDL) (Yu et al., 2008) and the WD-40 protein PLEIOTROPIC REGULATORY LOCUS1 (PRL1) (Zhang et al., 2014) bind pri-miRNAs to prevent their degradation.

To efficiently and accurately process pri-miRNAs, DCL1 forms a complex with the double-stranded RNA (dsRNA) binding protein HYPONASTIC LEAVES1 (HYL1), the zinc-finger protein SERRATE (SE), and the RNA binding protein TOUGH (TGH) (Fang and Spector, 2007; Fujioka et al., 2007; Song et al., 2007; Dong et al., 2008; Ren et al., 2012). The formation of the DCL1 complex requires NOT2 (Wang et al., 2013), ELONGATOR (Fang et al., 2015a), MODIFIER OF SNC1, 2 (MOS2; an RNA binding protein) (Wu et al., 2013), and the DEAH-box helicase PINP1 (Qiao et al., 2015). How MOS2 and PINP1 participate in the assembly of the DCL1 complex remains unclear, since they do not interact with the DCL1 complex (Wu et al., 2013; Qiao et al., 2015). Efficient loading of pri-miRNAs to the DCL1 complex requires TGH (Ren et al., 2012), the THO/TREX complex that is involved in nuclear RNA transport (Francisco-Mangilet et al., 2015), and the ribosome protein STV1 (Li et al., 2017). Notably,

[1] Address correspondence to byu3@unl.edu.
The author responsible for distribution of materials integral to the findings presented in this manuscript in accordance with the policy described in the Instructions for Authors (www.plantcell.org) is: Bin Yu (byu3@unl.edu).
www.plantcell.org/cgi/doi/10.1105/tpc.17.00953

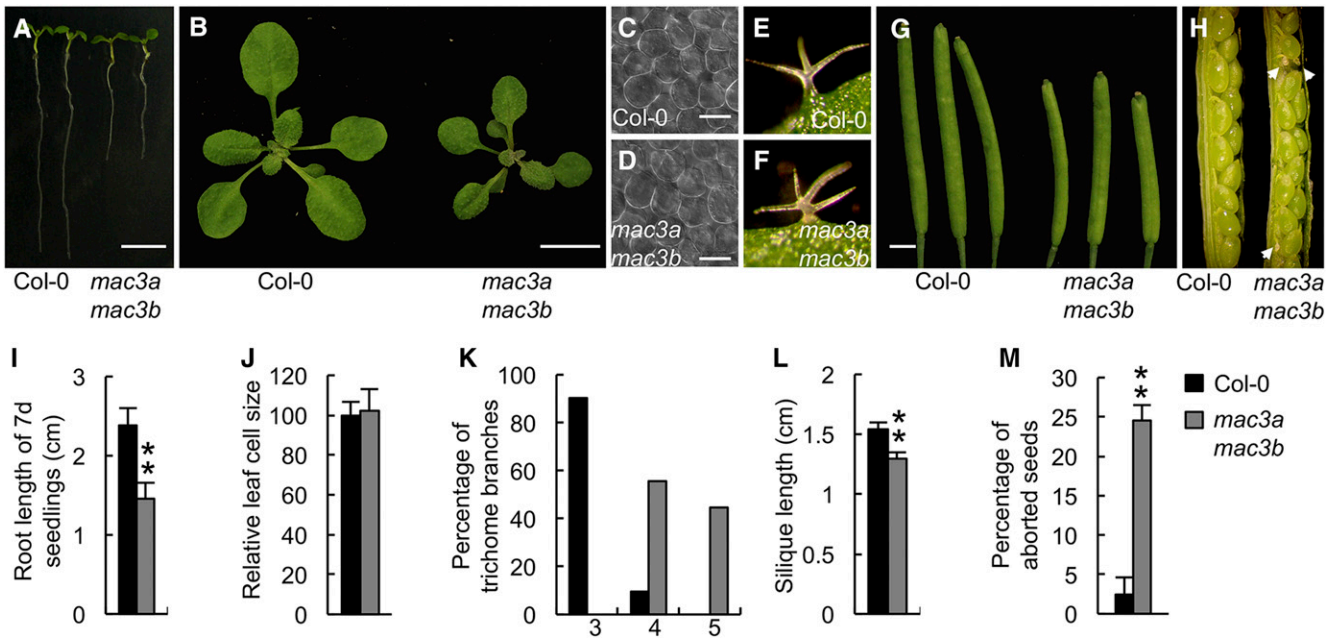

Figure 1. *mac3a mac3b* Displays Pleiotropic Developmental Defects.

(A) Seven-day-old seedlings of Col and *mac3a mac3b*. Bar = 5 mm.
(B) Three-week-old Col and *mac3a mac3b*. Bar = 1cm.
(C) and **(D)** Palisade cells of the fifth leaves from Col **(C)** and *mac3a mac3b* **(D)**. Bar = 100 μm.
(E) and **(F)** Trichomes of Col and *mac3a mac3b*. Bar = 0.3 mm.
(G) Mature siliques of Col and *mac3a mac3b.* Bar = 2mm.
(H) Dissected siliques of Col and *mac3a mac3b*. White arrow: aborted seeds.
(I) Quantification of root length in Col and *mac3a mac3b*. Thirty plants were measured to calculate average root length. **P < 0.01 by Student's *t* test.
(J) Quantification of cell size of the fifth leaves in Col and *mac3a mac3b*. The value of Col was set as 100. Eighty cells of the fifth leaves from each genotype were measured.
(K) Quantification of trichome branches in Col and *mac3a mac3b*. Sixty trichomes from each genotype were analyzed. Numbers (3, 4, or 5) indicate the number of branches.
(L) Quantification of silique length in Col and *mac3a mac3b*. Thirty siliques from the same position of each genotype were measured. **P < 0.01 by Student's *t* test.
(M) Quantification of aborted seeds in Col and *mac3a mac3b*. Twenty siliques from Col or *mac3a mac3b* were analyzed. **P < 0.01 by Student's *t* test, compared with Col-0 value. Error bars in **(I)** to **(M)** indicate SD.

several additional proteins, including the CAP BINDING PROTEINs (CBPs) (Gregory et al., 2008; Laubinger et al., 2008), NOT2, ELONGATOR, DDL, CDC5, and PRL1 also associate with the DCL1 complex to enhance pri-miRNA processing. In addition, SICKLE (SIC; a proline-rich protein) (Zhan et al., 2012), RECEPTOR FOR ACTIVATED C KINASE1 (RACK1) (Speth et al., 2013), STABILIZED1 (STA1; a pre-mRNA processing factor 6 homolog) (Ben Chaabane et al., 2013), REGULATOR OF CBF GENE EXPRESSION3 (RCF3; also known as HOS5 and SHI1) (Chen et al., 2015; Karlsson et al., 2015), and GRP7 (a glycine-rich RNA binding protein) (Köster et al., 2014) also regulate miRNA biogenesis. However, they do not associate with DCL1. Moreover, phosphorylation and dephosphorylation of HYL1 are crucial for pri-miRNA processing (Manavella et al., 2012). In addition, protein factors that act in miRNA biogenesis are also transcriptionally and posttranscriptionally regulated. For instance, DCL1 transcription is modulated by the histone acetyltransferase GCN5 (Kim et al., 2009), STA1 (Ben Chaabane et al., 2013), and the transcription factor XAP5 CIRCADIAN TIMEKEEPER (XCT) (Fang et al., 2015b). Notably, HYL1 protein levels are maintained by the SNF1-RELATED PROTEIN KINASE2 (Yan et al., 2017) and the E3 ubiquitin ligase CONSTITUTIVE PHOTOMORPHOGENIC1 (COP1) (Cho et al., 2014) through unknown mechanisms. Recently, KETCH1 (KARYOPHERIN ENABLING THE TRANSPORT OF THE CYTOPLASMIC HYL1)-mediated transportation of HYL1 from the cytoplasm to the nucleus was shown to be crucial for miRNA biogenesis (Zhang et al., 2017). Interestingly, pri-miRNA structures also influence the DCL1 activity (Mateos et al., 2010; Song et al., 2010; Werner et al., 2010; Bologna et al., 2013; Zhu et al., 2013). For instance, the internal loop below the miRNA/miRNA* within the stem-loop is important for the processing of some pri-miRNAs.

Among proteins associated with the DCL1 complex, CDC5 and PRL1 are two core subunits of the MOS4-assoicated complex (MAC) (Monaghan et al., 2009). MAC is a conserved complex that associates with the spliceosome (Deng et al., 2016). Its homolog

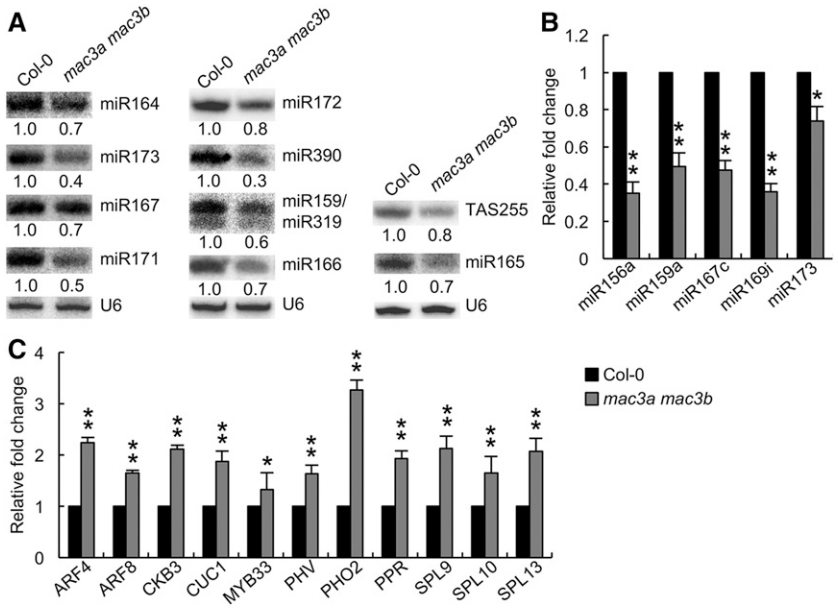

Figure 2. *mac3a mac3b* Reduces the Accumulation of miRNAs.

(A) The levels of small RNAs in Col and *mac3a mac3b* detected by RNA gel blot. *U6* RNA serves as the loading control. The numbers shown below the picture indicates the amount of small RNAs in *mac3a mac3* relative to that of Col (set as 1) and represent mean of three replicates ($P < 0.05$). miR159/319: the upper band was miR159 and the lower band showed miR319.

(B) The levels of miRNAs detected by RT-qPCR. miRNA levels in *mac3a mac3b* were normalized to those of *U6* RNA and compared with Col (value set as 1). Error bars indicate SD of three replicates (*$P < 0.05$ and **$P < 0.01$ by Student's *t* test, compared with Col-0 value).

(C) The transcript levels of miRNA targets in Col and *mac3a mac3b* detected by RT-qPCR. The transcript levels of miRNA targets were normalized to those of *UBIQUITIN5* (*UBQ5*) and compared with Col (set as 1). Error bars indicate SD of three replicates (**$P < 0.01$ by Student's *t* test, compared with Col-0 value).

complexes in human and yeast are known as the CDC5-SNEV$^{Prp19\text{-}Pso4}$ (PRP19) complex and the Nineteen complex (NTC), respectively (Palma et al., 2007). Both PRP19 and NTC function in splicing, DNA repair, the cell cycle, and genome stability (Chanarat and Straßer, 2013). MAC contains three additional core subunits, MAC3A, MAC3B, and MOS4, and at least 13 accessory proteins with diversified functions (Monaghan et al., 2009). Deficiency in MAC impairs plant immunity and development (Monaghan et al., 2009). However, related mechanisms still need investigation. We have previously shown that CDC5 and PRL1 have overlapping roles in regulating DCL1 activity, but distinct functions in pri-miRNA transcription and stability (Zhang et al., 2013, 2014). These results raise the possibility that other MAC components may also have diversified effects on miRNA biogenesis. Among core MAC components, MAC3A and MAC3B are two homologous U-box type E3 ubiquitin ligases (~82% identity and 90% similarity) (Monaghan et al., 2009). E3 ligase activity of MAC3B has been demonstrated in vitro (Wiborg et al., 2008). We previously showed that a loss-of-function mutation in MAC3A does not affect miRNA accumulation (Zhang et al., 2014). However, this result may reflect the redundant function of MAC3B with MAC3A.

In this study, we found that lack of both MAC3A and MAC3B reduces the accumulation of miRNAs and impairs the localization of HYL1 in the D-body. MAC3A associates with the DCL1 complex and pri-miRNAs and promotes pri-miRNA processing. MAC3A and MAC3B are also required for accumulation of pri-miRNAs. However, unlike CDC5, MAC3A neither interacts with Pol II nor affects *MIR* transcription. These results suggest that MAC3A/3B may stabilize pri-miRNAs and act as a cofactor to promote D-body formation and pri-miRNA processing. In addition, we show that MAC3A is a phosphorylation-dependent E3 ligase and its E3 ligase activity is required for miRNA biogenesis. We propose that MAC may act as a complex to promote miRNA biogenesis and different MAC components may have distinct and cooperative effects on pri-miRNA transcription, stability, and processing.

RESULTS

MAC3A and MAC3B Are Required for miRNA Biogenesis

The fact that CDC5 and PRL1, two core components of MAC, are required for miRNA biogenesis suggests that other MAC components may also function in miRNA biogenesis. However, we previously showed that a single *mac3a* mutation does not affect miRNA accumulation in *Arabidopsis thaliana* (Zhang et al., 2014). To evaluate if this result might reflect redundancy between MAC3A and MAC3B in miRNA biogenesis, we generated a *mac3a mac3b* double mutant through crossing *mac3a* (Salk_089300) to *mac3b* (Salk_050811) (Monaghan et al., 2009). Compared with Col (wild-type plant), *mac3a mac3b* displayed pleiotropic development defects (Figure 1). For instance, the root length of *mac3a mac3b* is much shorter (Figures 1A and 1I). Moreover, the size of the *mac3a mac3b* was smaller (Figure 1B). Reduced cell number was likely

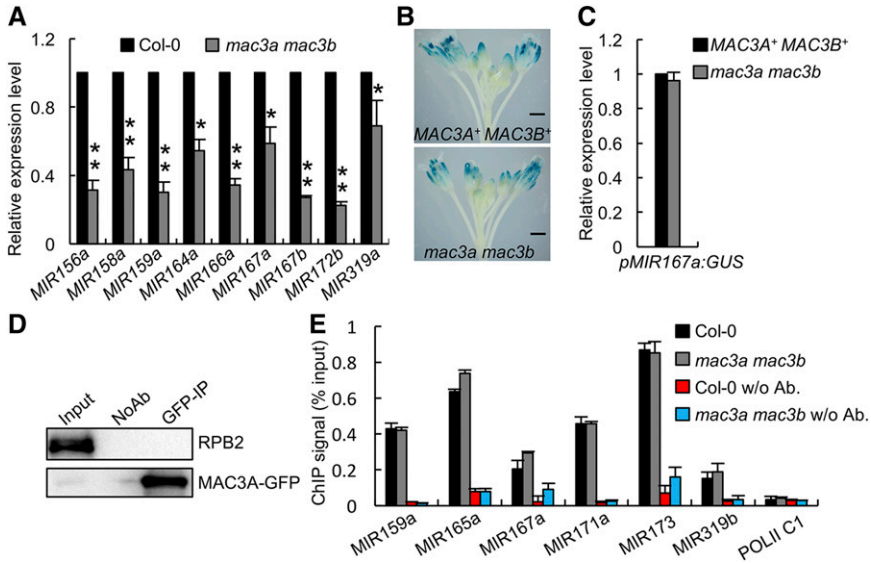

Figure 3. *mac3a mac3b* Reduces the Accumulation of pri-miRNAs without Affecting Transcription.

(A) The levels of pri-miRNAs in Col and *mac3a mac3b*. RT-qPCR was used to analyze pri-miRNA levels. pri-miRNA levels in *mac3a mac3b* were normalized to those of *UBQ5* and compared with Col (values were set as 1). Error bars indicate SD of three replicates (*P < 0.05 and **P < 0.01 by Student's *t* test, compared with Col-0 value).

(B) Histochemical staining of GUS in Col and *mac3a mac3b* harboring *proMIR167a:GUS*. Fifteen plants containing *GUS* were analyzed for each genotype. A representative image for each genotype is shown. Bar = 2 mm.

(C) *GUS* transcript levels in Col and *mac3a mac3b* harboring the *proMIR167a:GUS* transgene. *GUS* transcript levels detected by RT-qPCR were normalized to those of *UBQ5* and compared with Col (value was set as 1). Error bars indicate SD of three replicates.

(D) MAC3A does not coimmunoprecipitate with RPB2. Anti-GFP antibody was used to immunoprecipitate MAC3A-GFP. MAC3A-GFP and RPB2 were detected with anti-GFP and anti-RPB2 antibodies, respectively. Input, total proteins before IP; NoAb, immunoprecipitates with agarose beads.

(E) The occupancy of Pol II at *MIR* promoters in Col and *mac3a mac3b* detected by ChIP followed by qPCR. The intergenic region between At2g17470 and At2g17460 (POL II C1) was used as a negative control.

responsible for the smaller size of *mac3a mac3b*, since the size of palisade cells from *mac3a mac3b* was comparable to that from Col (Figures 1C, 1D, and 1J). In addition, *mac3a mac3b* leaves had three to four branch points (four to five branches) on average, while most trichomes of Col had two branch points (three branches) (Figures 1E, 1F, and 1K). Furthermore, the silique length of *mac3b mac3b* was shorter than that of Col (Figures 1G and 1L). Moreover, the amounts of aborted seeds were higher in the siliques of *mac3a mac3b* than those of the wild type (Figures 1H and 1M), suggesting that MAC3A and MAC3B also affect fertility.

The pleiotropic growth defects of *mac3a mac3b* are consistent with the effect of miRNAs on plant development; we therefore examined the accumulation of miRNAs in *mac3a mac3b* and Col through RNA gel blot. The abundance of all nine examined miRNAs was reduced in *mac3a mac3b* relative to Col (Figure 2A). RT-qPCR analyses further confirmed that miRNA levels were decreased in *mac3a mac3b* (Figure 2B). We also examined the effect of MAC3A and MAC3B on trans-acting siRNAs (ta-siRNAs), which is another class of sRNAs that represses gene expression at posttranscriptional levels (Peragine et al., 2004; Allen et al., 2005; Yoshikawa et al., 2005; Axtell et al., 2006). Similar to miRNAs, ta-siR255 was reduced in abundance in *mac3a mac3b* (Figure 2A). However, the effect MAC3A and 3B on ta-siR255 might be indirect, since the production of ta-siRNAs depending on miRNAs, whose abundance was reduced in *mac3a mac3b*.

We further compared miRNA profile from inflorescences of *mac3a mac3b* with that of the wild type through deep sequencing. The abundance of many miRNAs was reduced in *mac3a mac3b* relative to the wild type (Supplemental Figure 1A and Supplemental Data Set 1), suggesting that MAC3A MAC3B may have a global effect on miRNA accumulation. We also compared the effect of *mac3a mac3b* on miRNA accumulation with that of *dcl1-9* (a weak allele of *dcl* mutants) and *cdc5*. As expected, *cdc5* and *dcl1-9* reduced the abundance of most miRNAs (Supplemental Figures 1B and 1C and Supplemental Data Set 1). Among significantly down-regulated miRNAs (P < 0.1), DCL1, CDC5, and MAC3A/MAC3B showed overlapping effects on many of them (Supplemental Figure 1D). However, some miRNAs were differentially affected by DCL1, CDC5, and MAC3A/MAC3B (Supplemental Figure 1D). These results suggest that these proteins may have overlapping and distinct roles in miRNA biogenesis.

Next, we evaluated the influence of *mac3a mac3b* on the transcript levels of *ARF4*, *ARF8*, *CKB3*, *CUC1*, *MYB33*, *PHO2*, *PHV*, *PPR*, and *SPL9/10/13*, which are targets of tasiR-ARF, miR167, miR397, miR164, miR159, miR399, miR166, miR400, and miR156, respectively. The levels of these target transcripts were increased in *mac3a mac3b* compared with Col (Figure 2C), suggesting that MAC3A and 3B are required for optimal activity of miRNAs and ta-siRNAs.

To determine if the lack of MAC3A and MAC3B was responsible for the observed phenotypes, we expressed a genomic copy of

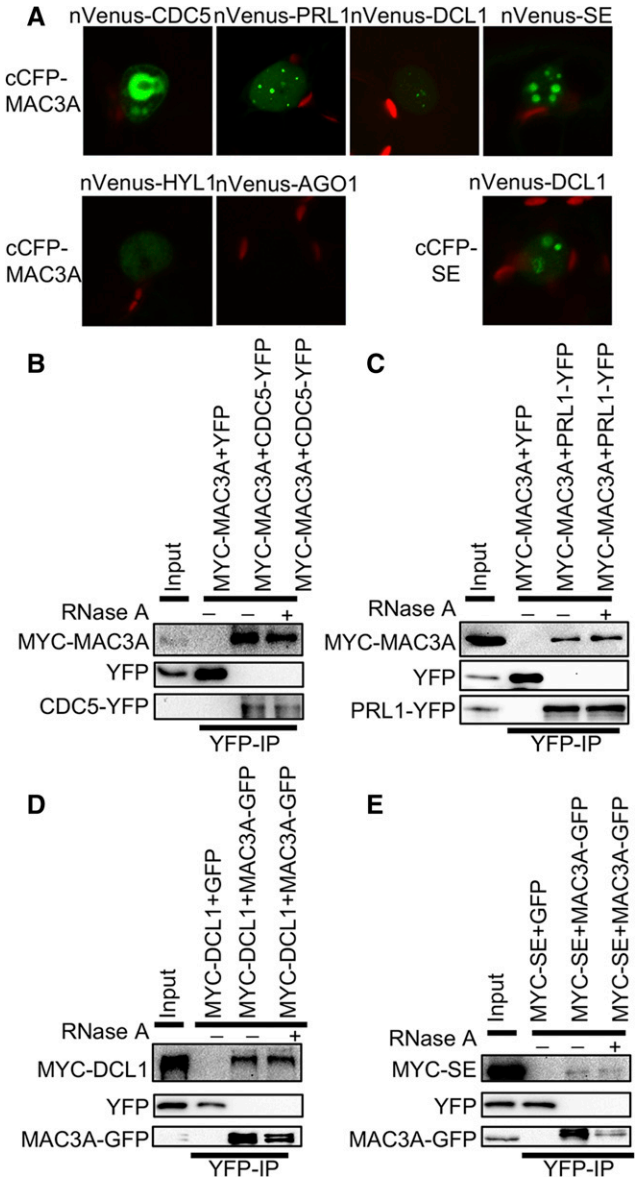

Figure 4. MAC3A Associates with the DCL1 Complex.

(A) The interaction of MAC3A with CDC5, PRL1, DCL1, HYL1, SE, and AGO1 detected by BiFC analysis. Paired cCFP- and nVenus-fusion proteins were coexpressed into *N. benthamiana* leaves. Green color indicates the BiFC signal (originally yellow fluorescence) detected by a confocal microscopy at 48 h after infiltration. One hundred nuclei were examined for each pair and a representative image is shown. Red: autofluorescence of chlorophyll.
(B) Co-IP between MAC3A and CDC5.
(C) Co-IP between MAC3A and PRL1. CDC5-YFP, PRL1-YFP or YFP were coexpressed with MYC-MAC3A in *N. benthamiana*. IP was performed using anti-YFP antibodies. MYC-MYC3A, CDC5-YFP, PRL1-YFP, and YFP were detected by immunoblot.
(D) Co-IP between MAC3A and DCL1.
(E) Co-IP between MAC3A and SE. GFP or MAC3A-GFP was coexpressed in *N. benthamiana* with MYC-DCL1 or MYC-SE, respectively. IP was performed using an anti-MYC antibody. After IP, proteins were detected by immunoblot. Inputs in **(B)** to **(E)** show the total protein before IP. RNase A was used to digest RNA stands.

MAC3A fused with a *GUS* gene at its 3′ end under the control of its native promoter (*proMAC3A:MAC3A-GUS*) in *mac3a mac3b*. The expression of this transgene rescued the developmental defects of *mac3a mac3b* (Supplemental Figure 2A). In addition, fusion constructs *MAC3B-GFP* (*pro35S:MAC3B-GFP*) or *MYC-MAC3A* (*pro35S:MYC-MAC3A*) under the control of the *35S* promoter also complemented the developmental defects of *mac3a mac3b* (Supplemental Figures 2B and 2J). Consistent with this observation, miRNA and target transcript levels in the complementation lines were comparable to those in Col (Supplemental Figures 2K and 2L). We also examined the expression pattern of MAC3A in *mac3a mac3b* harboring *proMAC3A:MAC3A-GUS* through GUS histochemical staining. MAC3A was universally expressed and displayed high expression levels in primary root tip, lateral root, and young leaves (Supplemental Figures 2C to 2I). These results demonstrate that MAC3A and MAC3B act redundantly to control development and miRNA accumulation of Arabidopsis.

MAC3A and MAC3B Do Not Affect *MIR* Transcription

We have previously shown that CDC5 and PRL1 regulate pri-miRNA levels through modulating pri-miRNA transcription and stability, respectively (Zhang et al., 2013, 2014). This led us to test if pri-miRNA levels were also altered in *mac3a mac3b*. As expected, all examined pri-miRNAs were reduced in abundance in *mac3a mac3b* compared with Col (Figure 3A). We suspected that as in *cdc5*, this reduction could be caused by alteration in transcription. Thus, we evaluated the effect of *mac3a mac3b* on *MIR* promoter activity. The *MIR* promoter reporter construct, *pMIR167a:GUS* (Zhang et al., 2014), was crossed into *mac3a mac3b*. Histochemical staining and RT-qPCR analyses revealed that the expression levels of GUS in *mac3a mac3b* were similar to those in the wild type (Figures 3B and 3C), indicating that MAC3A and MAC3B may have no effect on *MIR* promoter activity. Furthermore, we tested the interaction between MAC3A and the second largest subunit of Pol II (RPB2) through coimmunoprecipitation assay (co-IP) in the *mac3a mac3b* expression *pro35S:MAC3A-GFP*. In MAC3A-GFP precipitates, we did not detect the presence of RPB2 (Figure 3D), suggesting that unlike CDC5 and PRL1, MAC3A does not associate with RPB2. We also examined the occupancy of Pol II at the *MIR* promoters through chromatin immunoprecipitation (ChIP) assays in *mac3a mac3b* and Col performed using anti-RPB2 antibody. qPCR analysis did not detect an obvious difference of Pol II occupancy at various *MIR* promoters between *mac3a mac3b* and Col (Figure 3E). Taken together, these results suggest that MAC3A and MAC3B do not affect *MIR* transcription.

MAC3A and MAC3B Associate with the DCL1 Complex

To further understand how MAC3A and MAC3B affect miRNA biogenesis, we examined the effect of *mac3a mac3b* on the expression of *DCL1*, *DDL*, *SE*, *HYL1*, *CBP20/80*, and *HEN1*, which are known to function in miRNA biogenesis. The transcript levels of *HYL1* and *CBP20/80* were slightly increased, while the abundance of *DDL* transcripts was marginally reduced (Supplemental Figure 3A). In addition, the levels of *DCL1*, *HEN1*, and *SE* did not show significant change. Immunoblot analyses further showed that the protein levels of SE and DCL1 were not changed in *mac3a mac3b*,

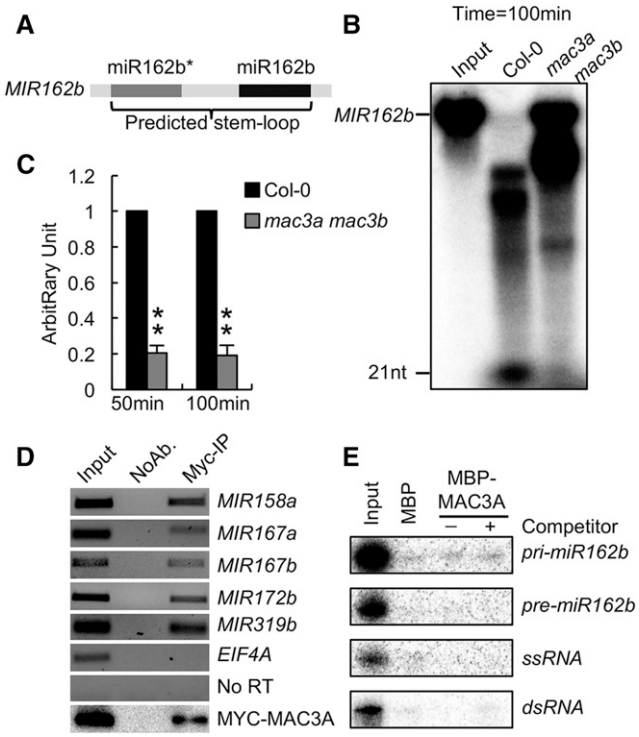

Figure 5. MAC3A Associates with pri-miRNAs and Promotes pri-miRNA Processing.

(A) Diagram of *MIR162b* used in the in vitro processing assay.
(B) *MIR162b* processing in protein extracts from *mac3a mac3b* and Col.
(C) Quantification of miR162 production in *mac3a mac3b* extracts relative to Col. The processing reaction was performed for 50 or 100 min. The radioactive signal of miR162 was normalized to input in *mac3a mac3b* and compared with that in Col (value set as 1). The value is the mean of three repeats. **P < 0.01 by Student's *t* test, compared with Col-0 value.
(D) MAC3A interacts with pri-miRNAs in vivo. RIP assay was performed on transgenic plants harboring *pro35S:MYC-MYC3A* using an anti-MYC antibody. Five percent RNAs were used as the input. NoAb: No antibody control.
(E) MAC3A does not bind RNAs in vitro. *pri-miR162b*, *pre-miR162b*, ssRNA, and dsRNA were generated through in vitro transcription.

whereas the HYL1 protein was slightly increased in abundance (Supplemental Figure 3B). Moreover, we also examined the effect of *mac3a mac3b* on the splicing of *DCL1*, *DDL*, *HEN1*, *HYL1*, and *SE* using RT-PCR with primers targeting a subset of introns (Supplemental Figure 3C). MAC3A and MAC3B did not have an obvious effect on the splicing of these introns (Supplemental Figures 3C and 3D). However, it is not clear if MAC3A and MAC3B affect the splicing of other introns in these examined genes.

Since MAC3A and MAC3B are components of the MAC, we suspected that like CDC5 and PRL1, MAC3A, and MAC3B might also interact with the DCL1 complex. We performed a bimolecular fluorescence complementation (BiFC) assay to test this possibility. In the leaves of *Nicotiana benthamiana* transiently coexpressing MAC3A or MAC3B fused with the C-terminal fragment of cyan fluorescent protein (cCFP) with CDC5, PRL1, DCL1, or SE fused with the N-terminal fragment of Venus (nVenus), yellow fluorescence signals were observed (shown in green color; Figure 4A; Supplemental Figure 4). BiFC signals of MAC3A or MAC3B with PRL1, DCL1, and SE were localized at the discrete bodies (Figure 4A; Supplemental Figure 4). Interestingly, the interaction between MAC3A/3B and CDC5 produced not only discrete signals but also diffused ones, agreeing with the role of MAC in mRNA splicing (Figure 4A; Supplemental Figure 4). Coexpression cCFP-MAC3A or cCFP-3B with nVenus-HYL1 resulted in weak and diffused YFP signals (Figure 4A; Supplemental Figure 4), consistent with the observation that CDC5 and PRL1 do not coimmunoprecipitate with HYL1 (Zhang et al., 2014).

Next, we used co-IP to confirm the interaction of MAC3A with CDC5, PRL1, DCL1, and SE. We first coexpressed MYC-MAC3A with CDC5-YFP, PRL1-YFP, or YFP and performed IP with anti-YFP antibodies. MYC3A was detected in CDC5-YFP and PRL1-YFP precipitates, but not in YFP precipitates (Figures 4B and 4C), confirming the interaction of MAC3A with CDC5 and PRL1. We next coexpressed MAC3A-GFP or GFP with MYC-DCL1 or MYC-SE and tested the interaction of coexpressed proteins. MAC3A-YFP, but not YFP, coimmunoprecipitated with MYC-DCL1 and MYC-SE (Figures 4D and 4E). Furthermore, RNase A treatment did not disrupt the interaction of MAC3A with DCL1 and SE (Figures 4B to 4D). These results suggest that MAC3A and MAC3B associate with the DCL1 complex in an RNA-independent manner.

mac3a mac3b Reduces pri-miRNA Processing in Vitro

The association of MAC3A and MAC3B suggests that they may modulate DCL1 activity. We used an in vitro pri-miRNA processing assay to test this possibility. As previously described, we first generated a radiolabeled pri-miR162b (*MIR162b*) composed of the stem-loop of miR162b with 6-nucleotide arms at each end using in vitro transcription (Figure 5A). Processing of *MIR162b* was then tested in the protein extracts from young flowers of *mac3a mac3b* or Col. The production of miR162b from *MIR162b* was reduced in the protein extracts of *mac3a mac3b* relative to Col (Figure 5B). At 50- and 100-min time points, the levels of miR162 generated in *mac3a mac3b* were ~20% of those produced in Col (Figure 5C). These results suggest that MAC3A/3B may be required for the optimal activity of the DCL1 complex.

MAC3A Binds pri-miRNAs in Vivo

The WD domain of MAC3A and MAC3B is known to mediate protein-protein interaction. However, it can also interact with RNAs (Lau et al., 2009). Thus, it is possible that MAC3A and MAC3B could bind pri-miRNAs. To test this hypothesis, we performed an RNA immunoprecipitation assay (RIP) on seedlings of the *mac3a mac3b* complementation line harboring the MYC-*MAC3A* transgene (Ren et al., 2012). Following cross-linking, nuclear isolation, and immunoprecipitation, we examined the presence of pri-miRNAs in MAC3A IPs using RT-PCR. All examined pri-miRNAs, but not the control *EIF4A* RNAs, were enriched in the MAC3A IPs (Figure 5D). By contrast, pri-miRNAs were not detected in the no-antibody controls (Figure 5D). These results suggest that MAC3A/3B associates with pri-miRNAs in vivo.

Next, we tested if MAC3A could directly bind pri-miRNA in vitro using the RNA pull-down assay (Ren et al., 2012). In this assay,

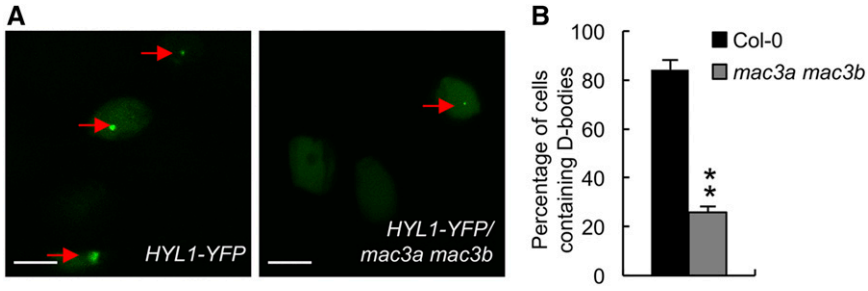

Figure 6. *mac3a mac3b* Affects the Localization of HYL1 in the Nucleus.

(A) Image of HYL1 localization in the root cells of Col and *mac3a mac3b*. Seven-day-old plants were examined. A typical image is shown. Arrows indicate the D-bodies. Bar = 5 μm.

(B) Quantification of root cells harboring HYL1-localized D-bodies in Col and *mac3a mac3b*. More than 400 cells from 12 roots for each genotype were examined. Error bar indicates SD (n = 400). **P < 0.01 by Student's t test, compared with Col-0 value.

MBP and recombinant MAC3A fused with maltose binding protein (MBP) at its N terminus (MBP-MAC3A) were expressed in *Escherichia coli*, purified with amylose resin, and then incubated with [^{32}P]-labeled *MIR162b* (Supplemental Figure 5A; Figure 5E). After washing, neither MBP-MAC3A nor MBP retained *MIR162b* (Figure 5E). MBP-MAC3A also did not interact with an ~100-nucleotide single-stranded RNA (ssRNA), which was generated through in vitro transcription using a N-terminal fragment of the *UBIQUITIN5* (*N-UBQ5*), or a dsRNA generated through annealing of sense and antisense strands of *N-UBQ5* (Figure 5E). Because MAC3A activity needs phosphorylation (see below), we treated the recombinant MAC3A protein with extracts from Col (see below) to modify the protein and then tested its interaction with *MIR162b*. The modified MAC3A also did not interact with RNAs (Supplemental Figure 5B). These results suggest that MAC3A is not an RNA binding protein.

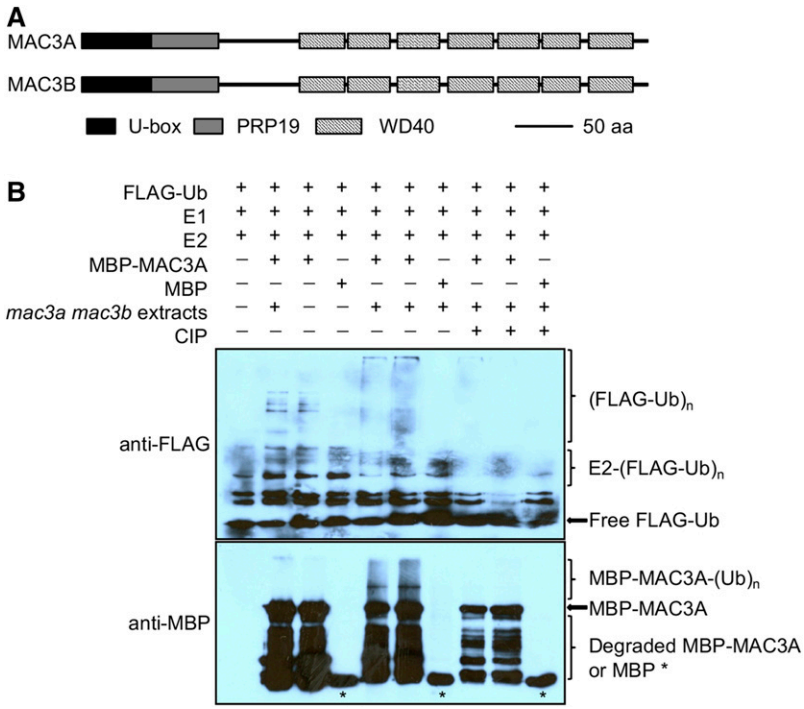

Figure 7. MAC3A Is a Bona Fide U-Box Ubiquitin E3 Ligase.

(A) The protein domains of MAC3A and MAC3B.

(B) Ubiquitin ligase activity of MAC3A. The in vitro ubiquitin ligase activity assay was performed in the presence of FLAG-ubiquitin (FLAG-Ub) and recombinant E1 and E2. MBP and no E3 ligase protein serve as negative controls. Polyubiquitination of MAC3A demonstrates its ubiquitin ligase activity. Anti-FLAG antibody and anti-MBP antibody were used to detect FLAG-ubiquitin and MBP/MBP-MAC3A, respectively. *mac3a mac3b* extracts: protein extracts from inflorescences of *mac3a mac3b*.

MAC3A and MAC3B Are Required for the Localization of HYL1 in D-Bodies

The interaction of MAC3A/B with the DCL1 complex also prompted us to test the effect of *mac3a mac3b* on the formation of the D-body. We crossed a HYL1-YFP transgenic line, which has been used as a reporter for the D-body (Wang et al., 2013; Wu et al., 2013; Qiao et al., 2015), into *mac3a mac3b* and examined the percentage of cells containing D-bodies in the root tips and elongation region. As previously reported (Wu et al., 2013), the HYL1-containing D-bodies existed in most cells (~84%; Figures 6A and 6B; Supplemental Figures 6A and 6B) in the wild type. By contrast, D-bodies were observed in only ~26% of cells in *mac3a mac3b*. This result demonstrates that MAC3A and MAC3B are required for correct HYL1 localization, indicating their potential role in facilitating D-body formation.

MAC3A Is a U-Box Ubiquitin E3 Ligase Whose Activity Depends on Phosphorylation

Both MAC3A and MAC3B contain an N-terminal ligase U-box domain that confers E3 ubiquitin ligase activity and recruits the E2 conjugating enzyme, a coiled-coil region that exists in all Prp19 homologs, mediates the tetramerization of Prp19 and interacts with CDC5L and SFP27 in metazoans, and a C-terminal WD domain composed of seven WD repeats that is required for substrate recruitment (Figure 7A). Homologous of MAC3A and MAC3B exist in all plants, while their copy numbers vary among different genomes (Supplemental Figure 7 and Supplemental Data Set 2).

Because MAC3A has considerable sequence difference from MAC3B, we tested if it is a ubiquitin E3 ligase using MBP-MAC3A (Supplemental Figure 5A). We examined the E3 ligase activity in the presence of ubiquitin, the ubiquitin-activating enzyme (E1) SlUBA, and the ubiquitin-conjugating enzyme (E2) UBC8 (Zhou et al., 2017). However, MBP-MAC3A displayed only weak activity (Figure 7B). We suspected that like some other E3 ligases, MAC3A activity might depend on posttranslational modification (Wang et al., 2015). Thus, we treated MBP-MAC3A and MBP protein with total protein extracts from inflorescences of *mac3a mac3b*. The use of *mac3a mac3b* was to avoid contamination from endogenous MAC3A/3B, since MAC3A potentially interacts with MAC3B. The treatment greatly improved MAC3A activity (Figure 7B). Notably, alkaline phosphatase (calf intestinal phosphatase [CIP]) treatment of MAC3A after incubation with *mac3a mac3b* protein extracts completely eliminated MAC3A activity (Figure 7B). These results demonstrate that MAC3A is a bona fide ubiquitin E3 ligase and that its activity depends on protein phosphorylation.

The Ubiquitin Ligase Activity of MAC3A Is Required for miRNA and pri-miRNA Accumulation

Since MAC3A is a ubiquitin ligase, we next asked if its function in miRNA biogenesis requires this activity. Based on the fact that the

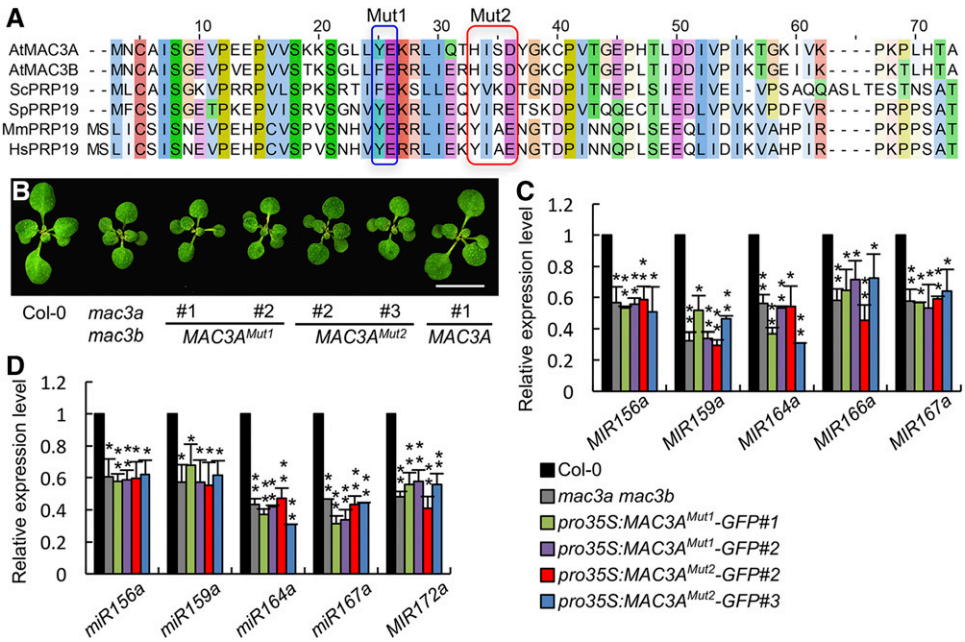

Figure 8. E3 Ubiquitin Ligase Activity Is Required for MAC3A Function in miRNA Biogenesis.

(A) The aligned sequences of conserved U-box domain in MAC3A orthologs. The two mutated sites are shown in blue and red boxes, respectively.
(B) Fourteen-day-old seedlings of Col, *mac3a mac3b*, and transgenic *mac3a mac3b* harboring *pro35S:MAC3A^{Mut1}-GFP* or *pro35S:MAC3A^{Mut2}-GFP* constructs. Two individual transgenic lines of each construct are shown. The transgenic line harboring *pro35S:MAC3A-GFP* is shown as control. Bar = 1 cm.
(C) and **(D)** The pri-miRNA **(C)** and miRNA **(D)** levels in Col, *mac3a mac3b*, *35S:MAC3A^{Mut1}-GFP* transgenic plants, and *pro35S:MAC3A^{Mut2}-GFP* transgenic plants detected by RT-qPCR. pri-miRNA levels in *mac3a mac3b* and transgenic plants were normalized to those of *UBQ5* and compared with Col (values were set as 1). miRNA levels in *mac3a mac3b* and transgenic plants were normalized to those of *U6* RNA and compared with Col (value set as 1). Error bars indicate SD of three replicates (*$P < 0.05$ and **$P < 0.01$ by Student's *t* test, compared with Col-0 value).

U-box domain of Prp19-like family is conserved in eukaryotes (Ohi et al., 2003), we generated two mutant versions of MAC3A in U-box domain through site-directed mutagenesis. In one mutant, the conserved amino acids of tyrosine (Y) at position 23 and glutamic acid (E) at position 24 were replaced with glycine (G) and alanine (A) (MAC3A^{Mut1}), respectively, while in the other one, the conserved amino acids of histidine (H) at position 31 and aspartic acid (D) at position 34 were replaced with alanines (AA) (MAC3A^{Mut2}) (Figure 8A). These two mutations disrupted the ubiquitin ligase activity of MAC3A (Supplemental Figure 8A). To evaluate the effect of MAC3A^{Mut1} and MAC3A^{Mut2} on miRNA biogenesis, we generated stable transgenic lines in *mac3a mac3b* expressing MAC3A^{Mut1} or MAC3A^{Mut2} under the control of 35S promoter. The expression MAC3A^{Mut1} or MAC3A^{Mut2} did not rescue the developmental defects of *mac3a mac3b* (Supplemental Figure 8B; Figure 8B). Agreeing with this observation, the accumulation of both pri-miRNAs and miRNAs in *mac3a mac3b* was not recovered by MAC3A^{Mut1} or MAC3A^{Mut2} (Figures 8C and 8D). These results suggest that the ubiquitin ligase activity of MAC3A is required for miRNA biogenesis.

DISCUSSION

MAC3A and MAC3B are conserved U-box type ubiquitin E3 ligases. In plants, MAC3A and MAC3B play important roles in plant immunity and development, and their counterparts in other organisms are required for splicing. In Arabidopsis, the MAC also associates with the spliceosome. However, only a few genes display moderated splicing in defects in *mac3a mac3b* (Monaghan et al., 2010; Xu et al., 2012). Consequently, how MAC3A and MAC3B regulate development and immunity remains elusive. In this study, we show that the accumulation of miRNA is reduced in *mac3a mac3b*. Furthermore, MAC3A and MAC3B associate with the DCL1 complex and pri-miRNAs. These results suggest that MAC3A and MAC3B are important players in miRNA biogenesis, in addition to their role in splicing. Impaired miRNA biogenesis may partially explain the pleiotropic developmental defects of *mac3a mac3b*, since miRNAs target many genes that are required for proper development.

There are at least three possible explanations for the decreased pri-miRNA levels in *mac3a mac3b*. First, *mac3a mac3b* may have reduced *MIR* transcription. The facts that *mac3a mac3b* does not show altered *MIR* promoter activity and that MAC3A does not co-IP with Pol II suggest that MAC3A and MAC3B may not affect *MIR* transcription. However, we cannot rule out the possibility that MAC3A and MAC3B influence *MIR* elongation or termination. Second, enhanced pri-miRNA processing in *mac3a mac3b* may also decrease pri-miRNA accumulation. However, reduced pri-miRNA processing is observed in *mac3a mac3b*, arguing against this possibility. Third, *mac3a mac3b* may have reduced stability of pri-miRNAs (Figure 9). We give this option more weight, given the observations that MAC3A associates with pri-miRNAs in vivo and interacts with PRL1, which protects pri-miRNAs from degradation. It is reasonable to speculate that MAC3A may stabilize pri-miRNAs through modulating the function of PRL1. Indeed, it has been observed that the interaction between PRP19 (a MAC3A ortholog) and the RNA binding protein

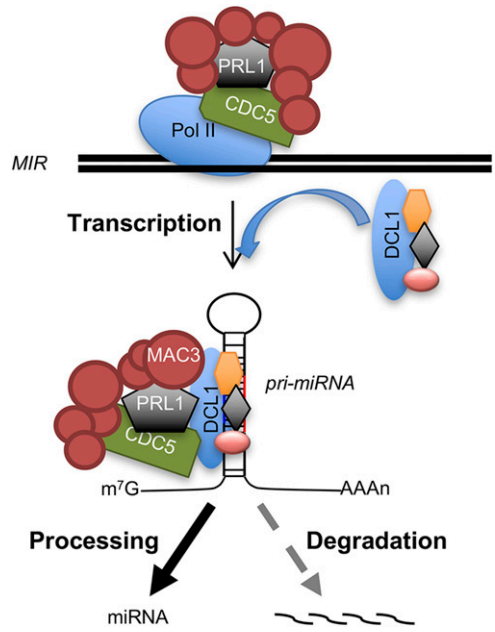

Figure 9. Proposed Model for MAC Function in miRNA Biogenesis.

MAC is required for pri-miRNA transcription, processing, and stability. Some MAC components such as CDC5 interact with the *MIR* promoter and Pol II to positively regulate *MIR* transcription. Following transcription, MAC binds pri-miRNAs to prevent their turnover and functions as a cofactor to promote pri-miRNA processing. The MAC may also facilitate the recruitment of the DCL1 complex to the processing sites. Because the MAC contains subunits with diversified functions, individual MAC components may contribute distinctly and synergistically to miRNA biogenesis. Lack of the MAC results in reduced pri-miRNA transcription, stability, and/or processing.

CWC2 is required for the stabilization of small nuclear RNAs related to splicing in yeast (McGrail et al., 2009; Vander Kooi et al., 2010).

MAC3A/MAC3B interacts with DCL1 and SE but appears to have weak or no association with HYL1. Interestingly, a lack of MAC3A and MAC3B impairs the localization of HYL1 at the D-body. How does this happen? One possibility is the decreased pri-miRNAs in *mac3a mac3b* may affect the formation of D-body. However, loss-of-function mutants *mos2* and *pinp1*, in which the levels of pri-miRNAs are increased or unaltered, respectively, also display impaired HYL1 localization or D-body assembly, arguing against this possibility. In human, PRP19-mediated ubiquitination regulates the protein-protein interaction of the spliceosome, which is important for the spliceosome assembly (Das et al., 2017). In addition, PRP19 also promotes the recruitment of ATRIP (a kinase) to the DNA damage site through modifying DNA replication protein A (Maréchal et al., 2014). Thus, it is possible that MAC3A and MAC3B may influence the recruitment of HYL1 through modifying proteins involved in D-body assembly. Alternatively, they may cotranscriptionally facilitate the recruitment of the D-body to the processing site of pri-miRNAs (Figure 9). The association of MAC3A/3B with the DCL1 complex is consistent with these hypotheses.

pri-miRNA processing is also reduced in *mac3a mac3b*. This cannot be attributed to altered expression of genes involved in miRNA biogenesis, as the levels of these genes are either slightly increased or unaltered in *mac3a mac3b*. We have shown the CDC5 promotes DCL1 activity through its interaction with the regulatory domains of DCL1 (Zhang et al., 2013), while PRL1 functions an accessory factor to facilitate CDC5 function in modulating DCL1 activity (Zhang et al., 2014). By analogy, MAC3A and MAC3B may function as components of the MAC to directly or indirectly enhance the DCL1 activity (Figure 9). Alternatively, impaired HYL1 localization or D-body formation may affect the DCL1 activity.

In summary, we find that MAC3A and MAC3B, two core components of the MAC, act redundantly in miRNA biogenesis. They associate with the DCL1 complex, positively modulate pri-miRNA accumulation, facilitate HYL1 localization at the D-body, and enhance DCL1 activity. More importantly, we show that MAC3A is a phosphorylation-dependent ubiquitin ligase and that this ligase activity is required for miRNA biogenesis. This result indicates that certain signals may modulate MAC3A activity through phosphorylation and thereby regulate miRNA accumulation. The involvement of four MAC core components in miRNA biogenesis suggests that the MAC functions as a complex to promote miRNA biogenesis.

Besides core components, the MAC also contains at least 13 accessory components. The core and accessory components of the MAC are proteins with diversified functions, such as transcription factors, RNA binding proteins, ubiquitin ligase, helicases, chromatin protein, WD proteins, protein-protein interaction regulators, coiled-coil domain-containing proteins, and zinc-finger-domain-containing proteins. Moreover, the accessory components are dynamically associated with the core complex, and subcomplexes with different functions are often formed. Thus, it is likely that various MAC components act individually and coordinately in miRNA biogenesis through influencing pri-miRNA transcription, processing, and stability and/or likely have a role in the assembly of D-body (Figure 9), which resembles the diversified function of PRP19 in splicing. Consistent with this notion, CDC5 and PRL1 contribute differently to pri-miRNA accumulation but act as a complex to regulate DCL1 activity. It will be interesting to further determine the functional mechanism of these proteins as individual components and as a complex in miRNA biogenesis. The functions of the PRP19 complex from metazoans in splicing, transcription, chromatin stability, and lipid droplet biogenesis have been well documented (Chanarat and Straßer, 2013). However, its function in metazoan miRNA biogenesis is unknown. Given the fact that all four MAC components associate with SE, an ortholog of ARS2, which is a key component of miRNA biogenesis in metazoa, it will not be surprising if the PRP19 complex plays a role in metazoan miRNA biogenesis.

METHODS

Plant Materials and Growth Conditions

SALK_089300 (*mac3a*) (Monaghan et al., 2009) and SALK_050811 (*mac3b*) were obtained from the ABRC. They are in the Columbia (Col) genetic background. Transgenic lines containing a single copy of *proMIR167a:GUS* or *pro35S:HYL1-YFP* were crossed to *mac3a mac3b*. In the F2 generation, wild-type plants or *mac3a mac3b* harboring *proMIR167a:GUS* or *pro35S:HYL1-YFP* were selected through PCR-based genotyping for *mac3a*, *mac3b*, *GUS*, or *GFP*. Approximately fifteen wild-type or *mac3a mac3b* plants were pooled for GUS transcript level analyses. All plants were grown at 22°C with 16-h-light (cool white fluorescent lamps, 25-W Sylvania 21942 FO25/741/ECO T8 linear tube) and 8-h-dark cycles.

Plasmid Construction

A DNA fragment containing 2066-bp promoter and 3841-bp coding region of *MAC3A* was PCR amplified using DNAs from Col as templates with the primers of proMAC3A-4F and MAC3Acds-1R. The resulting PCR product was cloned into pENTR/D-TOPO vector and subsequently cloned into pMDC163 binary vector to generate the *proMAC3A:MAC3A-GUS* plasmid. The *MAC3A* full-length cDNA was RT-PCR amplified with the primers of MAC3Acds-1F and MAC3Acds-1R, cloned into pENTR/D-TOPO vector, and subcloned into pEarleyGate203 or pMDC83 to generate the *pro35S:MYC-MAC3A* construct or the *pro35S:MAC3A-GFP* construct. The *MAC3B* full-length cDNA was amplified with the primers of MAC3Bcds-1F and MAC3Bcds-1R by RT-PCR and cloned into pENTR/D-TOPO vector and subcloned into pMDC83 to generate the *pro35S:MAC3B-GFP* construct. To construct *cCFP-MAC3A* or *cCFP-MAC3B*, *MAC3A* cDNA or *MAC3B* cDNA was PCR amplified using the primer pair MAC3A-3F/2R or MAC3B-3F/2R, respectively, and cloned into pSAT4-cCFP-C vector. Then, the *pro35S:cCFP-MAC3A* fragment or the *pro35S:cCFP-MAC3B* fragment was released by I-*Sce*I restriction enzyme digestion and subcloned to pPZP-RCS2-ocs-bar-RI vector. The constructs cCFP-SE, nVenus-DCL1, nVenus-HYL1, nVenus-SE, and nVenus-AGO1 were described previously (Ren et al., 2012). To construct *MBP-MAC3A*, the *MAC3A* cDNA sequence was amplified with primer MAC3A-5F(Not1) and MAC3A-5R(Sal1) and subsequently inserted into the pMAL-C5X vector. Site-mutagenesis of *MAC3A* was performed according the protocol of QuikChange II site-directed mutagenesis kit (Agilent). The primers are list in Supplemental Table 1.

Plant Complementation

The *proMAC3A:MAC3A-GUS*, *pro35S:MYC-MAC3A*, *pro35S:MAC3A^{Mut1}-GFP*, *pro35S:MAC3A^{Mut2}*-GFP, and *pro35S:MAC3B-GFP* plasmids were transformed into *mac3a mac3b* using *Agrobacterium tumefaciens*-mediated floral dip method. The transgenic plants harboring *proMAC3A:MAC3A-GUS*, *pro35S:MAC3A^{Mut1}-GFP*, *pro35S:MAC3A^{Mut2}*-GFP, or *pro35S:MAC3B-GFP* were selected on MS medium containing hygromycin (30 μg/mL). *pro35S:MYC-MAC3A* transformants were selected by spraying seedlings with 120 mg/L BASTA solution.

E3 Ubiquitin Ligase Activity Assay

MBP-tagged fusion proteins were expressed in *Escherichia coli* strain BL21 (DE3) and purified with Amylose Resin (E8021S; NEB) by following the protocol provided by the manufacturer. The purified proteins were further desalted and concentrated using the Amicon Centrifugal Filter (Millipore). The concentration of purified protein was determined using protein assay agent (Bio-Rad).

The in vitro ubiquitination assay was performed as described (Zhou et al., 2017). Briefly, the components of 3 μg FLAG-ubiquitin, 40 ng E1 (GST-SlUBA1), 120 ng 6xHIS-AtUBC8 with 4 μg MBP, MBP-MAC3A, MBP-MAC3A^{Mut1}, or MBP-MAC3A^{Mut2} proteins were added to a 30 μL reaction buffer (50 mM Tris-HCl, pH 7.5, 5 mM ATP, 5 mM $MgCl_2$, 2 mM DTT, 3 mM creatine phosphate, and 5 μg/mL creatine phosphokinase). To detect the influence of protein modification on MAC3A activity, the recombinant proteins were treated as previously described with modifications (Wang et al., 2015). Briefly, 4 μg MBP, MBP-MAC3A, MBP-MAC3A^{Mut1}, or MBP-MAC3A^{Mut2}-bound amylose resin were incubated with the total protein extracts from *mac3a mac3b* for 1 h at room temperature followed by

extensively washing for three times. Following treatment, half of protein-bound resin was treated with CIP (NEB) for 30 min, while the other half was incubated with reaction buffer without CIP. After washing, protein-bounded resins were used to perform ubiquitin assay as described above. The reaction was terminated by addition of SDS sample loading buffer with 100 mM DTT. FLAG-ubiquitin and MBP-MAC3A were then detected with a mouse monoclonal anti-FLAG M2-peroxidase-conjugated antibody (A8592; Sigma-Aldrich) and anti-MBP antibody (E8030; NEB), respectively.

Co-IP Assay

To test the interaction between MAC3A and RPB2, anti-RPB2 antibody was used to perform IP on the protein extracts from inflorescences of transgenic plants harboring *pro35S:MAC3A-GFP* (Ren et al., 2012). After IP, MAC3A-GFP and RPB2 were detected by immunoblot using an anti-GFP monoclonal antibody (B230720; Biolegend) and anti-RPB2 antibodies (ab10338; Abcam). To examine the co-IP of MAC3A with CDC5 and PRL1, MYC-MAC3A was coexpressed with YFP, CDC5-YFP, or PRL1-YFP in *Nicotiana benthamiana* as described (Ren et al., 2012). To examine the co-IP of MAC3A with DCL1 and SE, MAC3A-YFP was coexpressed with MYC-DCL1 or MYC-SE in *N. benthamiana.* IP was performed on protein extracts using anti-GFP or anti-MYC antibodies coupled to protein G agarose beads as described (Ren et al., 2012). After IP, proteins were detected with immunoblotting using monoclonal antibodies against YFP (B230720; Biolegend) or MYC (06-340; Millipore).

ChIP Assay

ChIP was performed using 14-d-old seedlings from Col-0 and *mac3a mac3b* as described (Kim et al., 2011). Three biological replicates were performed. Anti-RPB2 antibody (ab10338; Abcam) was used for immunoprecipitation. qPCR was performed using primers listed in Supplemental Table 1.

Dicer Activity Assay

In vitro MIR162b processing assay was performed as described (Qi et al., 2005; Ren et al., 2012). DNA templates used for in vitro transcription were generated through PCR with primers listed in Supplemental Table 1. In vitro transcription of *MIR162b*, *N-UBQ5*, and antisense *N-UBQ5* were performed using T7 RNA polymerase in the presence of [α-^{32}P]UTP, ATP, CTP, GTP, and unlabeled UTP. *MIR162b* was processed in reaction buffer (100 mM NaCl, 1 mM ATP, 0.2 mM GTP, 1.2 mM $MgCl_2$, 25 mM creatine phosphate, 30 μg/mL creatine kinase, and 4 units of RNase inhibitor) containing 30 μg protein at 25°C. After the reaction was stopped at 50 or 100 min, RNAs were extracted and separated on a PAGE gel. ImageQuant was used to quantify the radioactive signals detected by a phosphor imager.

Morphological Analyses and GUS Histochemical Staining

Morphological and cellular analyses were performed according to the previously reported methods (Li et al., 2012). GUS staining was performed as described (Zhang et al., 2013). Briefly, tissues from plants of *mac3a mac3b* harboring *proMAC3A:MAC3A-GUS* or plants harboring *proMIR167a:GUS* were incubated with staining solution at 37°C for 5 h. 70% ethanol was used for tissue clearing before imaging.

BiFC Assay

BiFC assay was performed as described (Zhang et al., 2013). Paired cCFP and nVenus fusion proteins were coexpressed in *N. benthamiana* leaves. After 40 h expression, a confocal microscope (Fluoview 500 workstation; Olympus) was used to detect YFP and chlorophyll autofluorescence signals at 488 nm with a narrow barrier (505–525 nm; BA505-525; Olympus).

RNA Gel Blot and RT-qPCR Analyses

RNA gel blotting was performed as described (Ren et al., 2012). Approximately fifteen micrograms of total RNAs extracted from inflorescences was resolved on 16% PAGE gel and transferred to nylon membranes. ^{32}P-labeled antisense DNA oligonucleotides were used to detect small RNAs. Radioactive signals were detected with a phosphor imager and quantified with ImageQuant. Inflorescences of plants grown on three different growth rooms at the same condition (22°C with 16-h-light and 8-h-dark cycles) were harvested as three replicates. The levels of pri-miRNAs, miRNA target transcripts, and GUS mRNA were determined using RT-qPCR. One microgram of total RNAs from inflorescences was used to generate cDNAs using the SuperScript III reverse transcriptase (Invitrogen) and an oligo dT18 primer. cDNAs were then used as templates for qPCR on an iCycler apparatus (Bio-Rad) with the SYBR green kit (Bio-Rad). The primers used for PCR are listed on Supplemental Table 1.

RIP Analyses

RIP was performed according to Wierzbicki et al. (2008) and Ren et al. (2012). Approximately two grams of seedlings of transgenic plants harboring the *pro35S:MYC-MAC3A* transgene was used to examine the association of MAC3A with pri-miRNAs in vivo. After cross-linking with 1% formaldehyde for 10 min, glycine was added to quench the reaction for 10 min. Nuclei were extracted and lysed in the buffer (50 mM Tris-HCl, pH 8.0, 10 mM EDTA, and 1% SDS) by sonication five times. After debris was removed by centrifugation at 16,000*g* for 10 min, equal amounts of proteins from various samples were diluted with RIP dilution buffer and incubated with anti-GFP antibodies conjugated to protein-G agarose beads. The immunoprecipitates were then eluted with elution buffer (100 mM $NaHCO_3$ and 1% SDS) at 65°C. Following reverse cross-linking with proteinase K (Invitrogen) and 200 mM NaCl at 65°C, RNAs were extracted and used as templates for RT-PCR analyses. All the primers are listed in Supplemental Table 1.

In Vitro RNA Pull-Down Assay

In vitro RNA pull-down assay was performed as described (Ren et al., 2012). The amylose resin beads containing MBP or MBP-MAC3A were incubated with [^{32}P]-labeled probes at 4°C for 1 h. After the beads were washed four times, RNAs were extracted and resolved on PAGE gels. Radioactive signals were detected with a phosphor Imager and quantified by ImageQuant.

Small RNA Sequencing

Inflorescences of Col, *mac3a mac3b*, and *cdc5-1* grown on two separate growth rooms at the same condition (22°C with 16-h-light and 8-h-dark cycles) were harvested as two biological replicates and used for RNA extraction and small RNA library preparation following standard protocol. The data set was deposited into the National Center for Biotechnology Information Gene Expression Omnibus (Col accession nos. GSM2829820 and GSM2829821; *mac3a mac3b* accession nos. GSM2829822 and GSM2829823; Col accession nos. GSM2805383 and GSM2805384; *cdc5-1* accession nos. GSM2805385 and GSM2805386). The sequencing data (Col access nos. GSM2257315, GSM2257316, and GSM2257317; *dcl1* accession nos. GSM2257321, GSM2257322, and GSM2257323) generated by Wu et al. (2016) were used to analyze the effect of DCL1 on miRNA accumulation. After sequencing, miRNA analysis was performed after removing reads aligned to t/r/sn/snoRNA according to Ren et al. (2012). Normalization was done using the total numbers of perfectly aligned reads (Nobuta et al., 2010). The mean values of miRNA abundance from biological replicates were compared by using EdgeR with trimmed mean of M values (TMM) normalization method (Robinson et al., 2010). Downregulated

miRNAs with confidence ($P < 0.1$; folder < 0.7) were used to identify the overlapping effect of *mac3a mac3b*, *cdc5-1*, and *dcl1-9*. The Venn diagram was plotted with the VennDiagram from the R package (Chen and Boutros, 2011).

Accession Numbers

Sequence data from this article can be found in the Arabidopsis Genome Initiative or GenBank/EMBL databases under the following accession numbers: *MAC3A* (AT1G04510), *MAC3B* (AT2G33340), *CDC5* (AT1G09770), *PRL1* (AT4G15900), *DCL1* (AT1G01040), *SE* (AT2G27100), *HYL1* (AT1G09700), *DDL* (AT3G20550), *CBP20* (AT5G44200), *CBP80* (AT2G13540), *HEN1* (AT4G20910), *AGO1* (AT1G48410), *ARF4* (AT5G60450), *ARF8* (AT5G37020), *CKB3* (AT3G60250), *CUC1* (AT3G15170), *MYB33* (AT5G06100), *PHV* (AT1G30490), *PHO2* (AT2G33770), *PPR* (AT1G62670), *SPL9* (AT2G42200), *SPL10* (AT1G27370), *SPL13* (AT5G50570), and *UBIQUITIN5* (AT3G62250). Protein sequences of MAC3 homologs in other species can be obtained in National Center for Biotechnology Information under the following accession numbers: AAN13133 (MAC3A, AT1G04510, *Arabidopsis thaliana*), FJ820118 (MAC3B, AT2G33340, Arabidopsis), XP_009143870 (*Brassica rapa*), XP_009141306 (*B. rapa*), XP_004247768 (*Solanum lycopersicum*), XP_003555746 (*Glycine max*), XP_003535988 (*G. max*), XP_015614850 (Os10g32880, *Oryza sativa*), KXG38386 (SORBI_3001G226000, *Sorghum bicolor*), ONM06005 (ZEAMMB73_Zm00001d032763, *Zea mays*), AQK65171 (ZEAMMB73_Zm00001d014078, *Z. mays*), XP_001701820 (*Chlamydomonas reinhardtii*), NP_055317 (HsPRP19, *Homo sapiens*), NP_598890 (MmPRP19, *Mus musculus*), CAB10135 (SpPRP19, *Shizosaccharomyces pombe*), and CAA97487 (ScPRP19, *Saccharomyces cerevisiae*). Small RNA deep sequencing data sets are available from the National Center for Biotechnology Information Gene Expression Omnibus under the following reference numbers: Col accession numbers GSM2829820 and GSM2829821; *mac3a mac3b* accession numbers GSM2829822 and GSM2829823; Col accession numbers GSM2805383 and GSM2805384, *cdc5-1* accession numbers GSM2805385 and GSM2805386; Col accession numbers GSM2257315, GSM2257316, and GSM2257317; *dcl1* accession numbers GSM2257321, GSM2257322, and GSM2257323.

Supplemental Data

Supplemental Figure 1. Small RNA sequencing analyses of *mac3a mac3b*, *cdc5* and *dcl1-9*.

Supplemental Figure 2. Expression of *MAC3A* and *MAC3B* complements the defects of *mac3a mac3b.*

Supplemental Figure 3. Effect of MAC3A and MAC3B on the expression levels and splicing of genes involved in miRNA biogenesis.

Supplemental Figure 4. Interaction of MAC3B with CDC5, PRL1, and the DCL1 complex detected by BiFC analysis.

Supplemental Figure 5. RNA binding activity of MAC3A.

Supplemental Figure 6. HYL1-YFP localization in root tips in Col and *mac3a mac3b* mutant.

Supplemental Figure 7. Phylogenetic analysis of MAC3A orthologs.

Supplemental Figure 8. Ubiquitin ligase activity of MAC3A is required for miRNA biogenesis.

Supplemental Table 1. The sequences of oligonucleotides.

Supplemental Data Set 1. miRNA profile change in *mac3a mac3b*, *cdc5-1*, and *dcl1-9* relative to wild-type plants as determined by small RNA sequencing.

Supplemental Data Set 2. Text file of the alignment used for the phylogenetic analysis shown in Supplemental Figure 7.

Supplemental Data Set 3. Results of statistical analyses.

ACKNOWLEDGMENTS

This work was supported by the Nebraska Soybean Board (Award 1727 to B.Y.), by the National Science Foundation (Awards OIA-1557417 to B.Y. and IOS-1645659 to L.Z.), and by the Pioneer Hundred Talents Program of Chinese Academy of Sciences (to S.L.).

AUTHOR CONTRIBUTIONS

S.L. and B.Y. designed the experiments and prepared the manuscript. S.L., B.Y., K.L., B.Z., M.L, S.Z., L.Z., and C.Z. performed the experiments. S.L., C.Z., and B.Y. analyzed the data.

Received December 12, 2017; revised January 16, 2018; accepted January 31, 2018; published February 5, 2018.

REFERENCES

Allen, E., Xie, Z., Gustafson, A.M., and Carrington, J.C. (2005). MicroRNA-directed phasing during trans-acting siRNA biogenesis in plants. Cell **121:** 207–221.

Axtell, M.J. (2013). Classification and comparison of small RNAs from plants. Annu. Rev. Plant Biol. **64:** 137–159.

Axtell, M.J., Jan, C., Rajagopalan, R., and Bartel, D.P. (2006). A two-hit trigger for siRNA biogenesis in plants. Cell **127:** 565–577.

Baulcombe, D. (2004). RNA silencing in plants. Nature **431:** 356–363.

Baumberger, N., and Baulcombe, D.C. (2005). Arabidopsis ARGONAUTE1 is an RNA Slicer that selectively recruits microRNAs and short interfering RNAs. Proc. Natl. Acad. Sci. USA **102:** 11928–11933.

Ben Chaabane, S., Liu, R., Chinnusamy, V., Kwon, Y., Park, J.H., Kim, S.Y., Zhu, J.K., Yang, S.W., and Lee, B.H. (2013). STA1, an Arabidopsis pre-mRNA processing factor 6 homolog, is a new player involved in miRNA biogenesis. Nucleic Acids Res. **41:** 1984–1997.

Bologna, N.G., Schapire, A.L., Zhai, J., Chorostecki, U., Boisbouvier, J., Meyers, B.C., and Palatnik, J.F. (2013). Multiple RNA recognition patterns during microRNA biogenesis in plants. Genome Res. **23:** 1675–1689.

Chanarat, S., and Sträßer, K. (2013). Splicing and beyond: the many faces of the Prp19 complex. Biochim. Biophys. Acta **1833:** 2126–2134.

Chen, H., and Boutros, P.C. (2011). VennDiagram: a package for the generation of highly-customizable Venn and Euler diagrams in R. BMC Bioinformatics **12:** 35.

Chen, T., Cui, P., and Xiong, L. (2015). The RNA-binding protein HOS5 and serine/arginine-rich proteins RS40 and RS41 participate in miRNA biogenesis in Arabidopsis. Nucleic Acids Res. **43:** 8283–8298.

Cho, S.K., Ben Chaabane, S., Shah, P., Poulsen, C.P., and Yang, S.W. (2014). COP1 E3 ligase protects HYL1 to retain microRNA biogenesis. Nat. Commun. **5:** 5867.

Das, T., Park, J.K., Park, J., Kim, E., Rape, M., Kim, E.E., and Song, E.J. (2017). USP15 regulates dynamic protein-protein interactions of the spliceosome through deubiquitination of PRP31. Nucleic Acids Res. **45:** 4866–4880.

Deng, X., Lu, T., Wang, L., Gu, L., Sun, J., Kong, X., Liu, C., and Cao, X. (2016). Recruitment of the NineTeen Complex to the activated spliceosome requires AtPRMT5. Proc. Natl. Acad. Sci. USA **113:** 5447–5452.

Dong, Z., Han, M.H., and Fedoroff, N. (2008). The RNA-binding proteins HYL1 and SE promote accurate in vitro processing of pri-miRNA by DCL1. Proc. Natl. Acad. Sci. USA **105:** 9970–9975.

Earley, K.W., and Poethig, R.S. (2011). Binding of the cyclophilin 40 ortholog SQUINT to Hsp90 protein is required for SQUINT function in Arabidopsis. J. Biol. Chem. **286:** 38184–38189.

Fang, X., Cui, Y., Li, Y., and Qi, Y. (2015a). Transcription and processing of primary microRNAs are coupled by Elongator complex in Arabidopsis. Nat. Plants **1:** 15075.

Fang, X., Shi, Y., Liu, X., Chen, Z., and Qi, Y. (2015b). CMA33/XCT regulates small RNA production through modulating the transcription of Dicer-like genes in Arabidopsis. Mol. Plant **8:** 1227–1236.

Fang, Y., and Spector, D.L. (2007). Identification of nuclear dicing bodies containing proteins for microRNA biogenesis in living Arabidopsis plants. Curr. Biol. **17:** 818–823.

Francisco-Mangilet, A.G., Karlsson, P., Kim, M.H., Eo, H.J., Oh, S.A., Kim, J.H., Kulcheski, F.R., Park, S.K., and Manavella, P.A. (2015). THO2, a core member of the THO/TREX complex, is required for microRNA production in Arabidopsis. Plant J. **82:** 1018–1029.

Fujioka, Y., Utsumi, M., Ohba, Y., and Watanabe, Y. (2007). Location of a possible miRNA processing site in SmD3/SmB nuclear bodies in Arabidopsis. Plant Cell Physiol. **48:** 1243–1253.

Gregory, B.D., O'Malley, R.C., Lister, R., Urich, M.A., Tonti-Filippini, J., Chen, H., Millar, A.H., and Ecker, J.R. (2008). A link between RNA metabolism and silencing affecting Arabidopsis development. Dev. Cell **14:** 854–866.

Hajheidari, M., Farrona, S., Huettel, B., Koncz, Z., and Koncz, C. (2012). CDKF;1 and CDKD protein kinases regulate phosphorylation of serine residues in the C-terminal domain of Arabidopsis RNA polymerase II. Plant Cell **24:** 1626–1642.

Karlsson, P., Christie, M.D., Seymour, D.K., Wang, H., Wang, X., Hagmann, J., Kulcheski, F., and Manavella, P.A. (2015). KH domain protein RCF3 is a tissue-biased regulator of the plant miRNA biogenesis cofactor HYL1. Proc. Natl. Acad. Sci. USA **112:** 14096–14101.

Kim, W., Benhamed, M., Servet, C., Latrasse, D., Zhang, W., Delarue, M., and Zhou, D.X. (2009). Histone acetyltransferase GCN5 interferes with the miRNA pathway in Arabidopsis. Cell Res. **19:** 899–909.

Kim, Y.J., Zheng, B., Yu, Y., Won, S.Y., Mo, B., and Chen, X. (2011). The role of Mediator in small and long noncoding RNA production in *Arabidopsis thaliana*. EMBO J. **30:** 814–822.

Köster, T., Meyer, K., Weinholdt, C., Smith, L.M., Lummer, M., Speth, C., Grosse, I., Weigel, D., and Staiger, D. (2014). Regulation of pri-miRNA processing by the hnRNP-like protein AtGRP7 in Arabidopsis. Nucleic Acids Res. **42:** 9925–9936.

Lau, C.K., Bachorik, J.L., and Dreyfuss, G. (2009). Gemin5-snRNA interaction reveals an RNA binding function for WD repeat domains. Nat. Struct. Mol. Biol. **16:** 486–491.

Laubinger, S., Sachsenberg, T., Zeller, G., Busch, W., Lohmann, J.U., Rätsch, G., and Weigel, D. (2008). Dual roles of the nuclear cap-binding complex and SERRATE in pre-mRNA splicing and microRNA processing in *Arabidopsis thaliana*. Proc. Natl. Acad. Sci. USA **105:** 8795–8800.

Li, S., Liu, K., Zhang, S., Wang, X., Rogers, K., Ren, G., Zhang, C., and Yu, B. (2017). STV1, a ribosomal protein, binds primary microRNA transcripts to promote their interaction with the processing complex in Arabidopsis. Proc. Natl. Acad. Sci. USA **114:** 1424–1429.

Li, S., Liu, Y., Zheng, L., Chen, L., Li, N., Corke, F., Lu, Y., Fu, X., Zhu, Z., Bevan, M.W., and Li, Y. (2012). The plant-specific G protein γ subunit AGG3 influences organ size and shape in *Arabidopsis thaliana*. New Phytol. **194:** 690–703.

Manavella, P.A., Hagmann, J., Ott, F., Laubinger, S., Franz, M., Macek, B., and Weigel, D. (2012). Fast-forward genetics identifies plant CPL phosphatases as regulators of miRNA processing factor HYL1. Cell **151:** 859–870.

Maréchal, A., Li, J.M., Ji, X.Y., Wu, C.S., Yazinski, S.A., Nguyen, H.D., Liu, S., Jiménez, A.E., Jin, J., and Zou, L. (2014). PRP19 transforms into a sensor of RPA-ssDNA after DNA damage and drives ATR activation via a ubiquitin-mediated circuitry. Mol. Cell **53:** 235–246.

Mateos, J.L., Bologna, N.G., Chorostecki, U., and Palatnik, J.F. (2010). Identification of microRNA processing determinants by random mutagenesis of Arabidopsis MIR172a precursor. Curr. Biol. **20:** 49–54.

McGrail, J.C., Krause, A., and O'Keefe, R.T. (2009). The RNA binding protein Cwc2 interacts directly with the U6 snRNA to link the nineteen complex to the spliceosome during pre-mRNA splicing. Nucleic Acids Res. **37:** 4205–4217.

Monaghan, J., Xu, F., Xu, S., Zhang, Y., and Li, X. (2010). Two putative RNA-binding proteins function with unequal genetic redundancy in the MOS4-associated complex. Plant Physiol. **154:** 1783–1793.

Monaghan, J., Xu, F., Gao, M., Zhao, Q., Palma, K., Long, C., Chen, S., Zhang, Y., and Li, X. (2009). Two Prp19-like U-box proteins in the MOS4-associated complex play redundant roles in plant innate immunity. PLoS Pathog. **5:** e1000526.

Nobuta, K., McCormick, K., Nakano, M., and Meyers, B.C. (2010). Bioinformatics analysis of small RNAs in plants using next generation sequencing technologies. Methods Mol. Biol. **592:** 89–106.

Ohi, M.D., Vander Kooi, C.W., Rosenberg, J.A., Chazin, W.J., and Gould, K.L. (2003). Structural insights into the U-box, a domain associated with multi-ubiquitination. Nat. Struct. Biol. **10:** 250–255.

Palma, K., Zhao, Q., Cheng, Y.T., Bi, D., Monaghan, J., Cheng, W., Zhang, Y., and Li, X. (2007). Regulation of plant innate immunity by three proteins in a complex conserved across the plant and animal kingdoms. Genes Dev. **21:** 1484–1493.

Peragine, A., Yoshikawa, M., Wu, G., Albrecht, H.L., and Poethig, R.S. (2004). SGS3 and SGS2/SDE1/RDR6 are required for juvenile development and the production of trans-acting siRNAs in Arabidopsis. Genes Dev. **18:** 2368–2379.

Qi, Y., Denli, A.M., and Hannon, G.J. (2005). Biochemical specialization within Arabidopsis RNA silencing pathways. Mol. Cell **19:** 421–428.

Qiao, Y., Shi, J., Zhai, Y., Hou, Y., and Ma, W. (2015). Phytophthora effector targets a novel component of small RNA pathway in plants to promote infection. Proc. Natl. Acad. Sci. USA **112:** 5850–5855.

Ren, G., Chen, X., and Yu, B. (2014). Small RNAs meet their targets: when methylation defends miRNAs from uridylation. RNA Biol. **11:** 1099–1104.

Ren, G., Xie, M., Dou, Y., Zhang, S., Zhang, C., and Yu, B. (2012). Regulation of miRNA abundance by RNA binding protein TOUGH in Arabidopsis. Proc. Natl. Acad. Sci. USA **109:** 12817–12821.

Robinson, M.D., McCarthy, D.J., and Smyth, G.K. (2010). edgeR: a Bioconductor package for differential expression analysis of digital gene expression data. Bioinformatics **26:** 139–140.

Smith, M.R., Willmann, M.R., Wu, G., Berardini, T.Z., Möller, B., Weijers, D., and Poethig, R.S. (2009). Cyclophilin 40 is required for microRNA activity in Arabidopsis. Proc. Natl. Acad. Sci. USA **106:** 5424–5429.

Song, L., Axtell, M.J., and Fedoroff, N.V. (2010). RNA secondary structural determinants of miRNA precursor processing in Arabidopsis. Curr. Biol. **20:** 37–41.

Song, L., Han, M.H., Lesicka, J., and Fedoroff, N. (2007). Arabidopsis primary microRNA processing proteins HYL1 and DCL1 define a nuclear body distinct from the Cajal body. Proc. Natl. Acad. Sci. USA **104:** 5437–5442.

Speth, C., Willing, E.M., Rausch, S., Schneeberger, K., and Laubinger, S. (2013). RACK1 scaffold proteins influence miRNA abundance in Arabidopsis. Plant J. **76:** 433–445.

Vander Kooi, C.W., Ren, L., Xu, P., Ohi, M.D., Gould, K.L., and Chazin, W.J. (2010). The Prp19 WD40 domain contains

a conserved protein interaction region essential for its function. Structure **18:** 584–593.

Vaucheret, H. (2008). Plant ARGONAUTES. Trends Plant Sci. **13:** 350–358.

Voinnet, O. (2009). Origin, biogenesis, and activity of plant microRNAs. Cell **136:** 669–687.

Wang, J., et al. (2015). The E3 ligase OsPUB15 interacts with the receptor-like kinase PID2 and regulates plant cell death and innate immunity. BMC Plant Biol. **15:** 49.

Wang, L., Song, X., Gu, L., Li, X., Cao, S., Chu, C., Cui, X., Chen, X., and Cao, X. (2013). NOT2 proteins promote polymerase II-dependent transcription and interact with multiple microRNA biogenesis factors in Arabidopsis. Plant Cell **25:** 715–727.

Werner, S., Wollmann, H., Schneeberger, K., and Weigel, D. (2010). Structure determinants for accurate processing of miR172a in Arabidopsis thaliana. Curr. Biol. **20:** 42–48.

Wiborg, J., O'Shea, C., and Skriver, K. (2008). Biochemical function of typical and variant Arabidopsis thaliana U-box E3 ubiquitin-protein ligases. Biochem. J. **413:** 447–457.

Wierzbicki, A.T., Haag, J.R., and Pikaard, C.S. (2008). Noncoding transcription by RNA polymerase Pol IVb/Pol V mediates transcriptional silencing of overlapping and adjacent genes. Cell **135:** 635–648.

Wu, C., Li, X., Guo, S., and Wong, S.M. (2016). Analyses of RNA-Seq and sRNA-Seq data reveal a complex network of anti-viral defense in TCV-infected *Arabidopsis thaliana*. Sci. Rep. **6:** 36007.

Wu, X., Shi, Y., Li, J., Xu, L., Fang, Y., Li, X., and Qi, Y. (2013). A role for the RNA-binding protein MOS2 in microRNA maturation in Arabidopsis. Cell Res. **23:** 645–657.

Xie, Z., Allen, E., Fahlgren, N., Calamar, A., Givan, S.A., and Carrington, J.C. (2005). Expression of Arabidopsis MIRNA genes. Plant Physiol. **138:** 2145–2154.

Xu, F., Xu, S., Wiermer, M., Zhang, Y., and Li, X. (2012). The cyclin L homolog MOS12 and the MOS4-associated complex are required for the proper splicing of plant resistance genes. Plant J. **70:** 916–928.

Yan, J., et al. (2017). The SnRK2 kinases modulate miRNA accumulation in Arabidopsis. PLoS Genet. **13:** e1006753.

Yoshikawa, M., Peragine, A., Park, M.Y., and Poethig, R.S. (2005). A pathway for the biogenesis of trans-acting siRNAs in Arabidopsis. Genes Dev. **19:** 2164–2175.

Yu, B., Bi, L., Zheng, B., Ji, L., Chevalier, D., Agarwal, M., Ramachandran, V., Li, W., Lagrange, T., Walker, J.C., and Chen, X. (2008). The FHA domain proteins DAWDLE in Arabidopsis and SNIP1 in humans act in small RNA biogenesis. Proc. Natl. Acad. Sci. USA **105:** 10073–10078.

Zhai, J., et al. (2013). Plant microRNAs display differential 3′ truncation and tailing modifications that are ARGONAUTE1 dependent and conserved across species. Plant Cell **25:** 2417–2428.

Zhan, X., Wang, B., Li, H., Liu, R., Kalia, R.K., Zhu, J.K., and Chinnusamy, V. (2012). Arabidopsis proline-rich protein important for development and abiotic stress tolerance is involved in microRNA biogenesis. Proc. Natl. Acad. Sci. USA **109:** 18198–18203.

Zhang, S., Liu, Y., and Yu, B. (2014). PRL1, an RNA-binding protein, positively regulates the accumulation of miRNAs and siRNAs in Arabidopsis. PLoS Genet. **10:** e1004841.

Zhang, S., Liu, Y., and Yu, B. (2015). New insights into pri-miRNA processing and accumulation in plants. Wiley Interdiscip. Rev. RNA **6:** 533–545.

Zhang, S., Xie, M., Ren, G., and Yu, B. (2013). CDC5, a DNA binding protein, positively regulates posttranscriptional processing and/or transcription of primary microRNA transcripts. Proc. Natl. Acad. Sci. USA **110:** 17588–17593.

Zhang, Z., Guo, X., Ge, C., Ma, Z., Jiang, M., Li, T., Koiwa, H., Yang, S.W., and Zhang, X. (2017). KETCH1 imports HYL1 to nucleus for miRNA biogenesis in Arabidopsis. Proc. Natl. Acad. Sci. USA **114:** 4011–4016.

Zhou, B., Mural, R.V., Chen, X., Oates, M.E., Connor, R.A., Martin, G.B., Gough, J., and Zeng, L. (2017). A subset of ubiquitin-conjugating enzymes is essential for plant immunity. Plant Physiol. **173:** 1371–1390.

Zhu, H., Zhou, Y., Castillo-González, C., Lu, A., Ge, C., Zhao, Y.T., Duan, L., Li, Z., Axtell, M.J., Wang, X.J., and Zhang, X. (2013). Bidirectional processing of pri-miRNAs with branched terminal loops by Arabidopsis Dicer-like1. Nat. Struct. Mol. Biol. **20:** 1106–1115.